Progress in Nuclear Energy 52 (2010) 435–441

Contents lists available at ScienceDirect

Progress in Nuclear Energy

journal homepage: www.elsevier.com/locate/pnucene

# Solid-solid conductance in nuclear fuel: An assessment of it in-code models performance

L.E. Herranz [a], A. Tigeras [b,*]

[a] Unit of Nuclear Safety Research, CIEMAT, 28040 Madrid, Spain
[b] EDF, 2 rue Ampère, 93206 Saint Denis cedex 01, France

*Keywords:*
Nuclear fuel
Heat transfer
Fuel-rod performance codes
Solid-solid conductance

A B S T R A C T

In the nuclear industry the preservation of cladding integrity should be always ensured under any expected or unexpected event. Given the current trend towards higher fuel burn-up, conditions of fuel-rod performance are becoming more demanding and, at the same time, safety assessments are moving from a conservative to a best-estimate approach, where more accurate models are used to reduce too large conservative margins. Heat transfer from the fuel rod plays an essential role for an accurate description of fuel performance.

The present paper is focused on heat transfer from the fuel to the inner side of the cladding under high burn-up conditions. Fundamentals of fuel-to-clad heat transfer and their implementation in "steady-state" performance codes have been reviewed. Major variables in the process have been identified (burn-up, pressure contact, interfacial temperature, morphology), and the main hypotheses and approximations used in each code to estimate them, have been examined and compared. Finally, model predictions have been compared to experimental data taken from the open literature. Even though the reduced number of data does not allow to settle general conclusions about model performance, substantial discrepancies have been found in their predictions. They have highlighted two important facts: the large scattering of already available data base and the scarcity of data under anticipated high burn-up conditions.



## 1. Introduction

Search for optimising electric unit cost in a growing power deregulation market has enhanced the trend towards higher fuel burn-up in the nuclear industry. This would require extension of current cycle lengths and/or power upgrading. As a consequence, conditions of fuel-rod performance would be more demanding and preservation of cladding integrity should be ensured under any expected or unexpected event. At the same time, safety assessments are moving from a conservative approach where large margins are taken on the safe side of hypotheses and approximations to accommodate uncertainties, to a best-estimate approach where more accurate models are used to reduce too large conservative margins.

Modelling of fuel thermal performance is particularly important since it would be breakdown of heat generation and transfer trade-off the triggering of an accidental situation. Traditionally, it consists of two major equations: a steady state solution of heat diffusion equation within fuel rod and an energy balance between in-rod generation and transfer from fuel surface. Heat passes from rod to coolant through the fuel-to-clad gap and the cladding. Recently, some of the hypotheses and approximations made concerning heat transfer through the fuel cladding were reviewed and assessed by Herranz et al. (2003).

The present paper is focused on heat transfer from the fuel to the inner side of the cladding under high burn-up conditions. Fundamentals of fuel-to-clad heat transfer and their implementation in "steady-state" performance codes have been reviewed. Major variables in the process have been identified and the main hypotheses and approximations used in each code to estimate them, have been examined and compared. Finally, model predictions have been compared to experimental data taken from the open literature and some conclusions have been stated.

## 2. Heat transfer scenario

### 2.1. Total thermal resistance

In a Light Water nuclear Reactor (LWR) fuel-to-coolant heat transfer is a traditional scenario of cylindrical topology with internal heat generation. By solving the general heat diffusion

* Corresponding author. Tel.: +33 (0) 1 43 69 73 55/33 663688774; fax: +33 (0) 1 43 69 82 93.
*E-mail address:* arancha.tigeras@edf.fr (A. Tigeras).

0149-1970/$ – see front matter © 2009 Elsevier Ltd. All rights reserved.
doi:10.1016/j.pnucene.2009.09.018

equation under steady state conditions, one can get the following expression of the temperature profile across the fuel rod:

$$T(r) = -\frac{\dot{q}'}{4k_{\text{fuel}}A_{\text{fuel}}}\left(r_{\text{fuel}}^2 - r^2\right) + R_{\text{Total}}\cdot\dot{q}'\cdot L + T_{\text{cool}} \quad (1)$$

In other words, fuel temperature is dependent upon linear heat rate generation ($\dot{q}'$), coolant temperature and total thermal resistance ($R_{\text{Total}}$). Both heat rate generation and coolant temperature are control variables of the reactor. However, the total thermal resistance,

$$R_{\text{Total}} = R_{\text{gap}} + R_{\text{Zry}} + R_{\text{oxide}} + R_{\text{cool}} \quad (2)$$

evolves naturally in the reactor environment during irradiation. For instance, water is capable of reacting with the metallic cladding and forms an oxide layer ($R_{\text{oxide}}$) that grows continuously while the cladding thermal resistance ($R_{\text{Zry}}$) decreases due to the clad thinning. The generic thermal resistance scheme is displayed in Fig. 1.

Herranz et al. (2003) studied the evolution of the above thermal resistances in a fuel rod irradiated up to 68 GWd/tU under typical reactor operation conditions. They showed that $R_{\text{Total}}$ is dominated at the beginning of the irradiation (until gap closure) by the $R_{\text{gap}}$ and, once the gap is closed, $R_{\text{gap}}$ becomes dominant again at burn-ups around 50 GWd/tU (gap conductivity reduction). Fig. 2 illustrates these results.

### 2.2. Gap thermal resistance

In terms of thermal conductance ($h$), the gap heat transfer can be described by:

$$h_{\text{gap}} = h_{\text{solid}} + h_{\text{gas}} \quad (3)$$

So to say, even though heat transfer from the outer surface of fuel to the inner side of the cladding occurs simultaneously by radiation, solid-to-solid contact and through the fluid, some approximations can be made. Convection is considered negligible because of the small gap width (around 50–10 μm) that makes gas to move extremely slow (Godesar, 1972). Radiation is disregarded because under normal operation conditions it is responsible for less than 1% of the transfer (Lasmann and Pazdera, 1983).

The gap thermal conductance also evolves due to the changes induced by irradiation. At the beginning of irradiation, when the gap is opened, $h_{\text{gap}}$ can be calculated by:

$$h_{\text{gap}} = h_{\text{gas}} = \frac{k_{\text{gas}}}{\delta} \quad (4)$$

where $\delta$ is the gap width. From then on, fuel swelling and relocation and clad creep narrow the gap till both materials contact each other, so that heat transfer evolves from heat transfer through a gas layer to a classical contact thermal conduction through solid contact spots ($h_{\text{solid}}$) and through gaseous gaps.

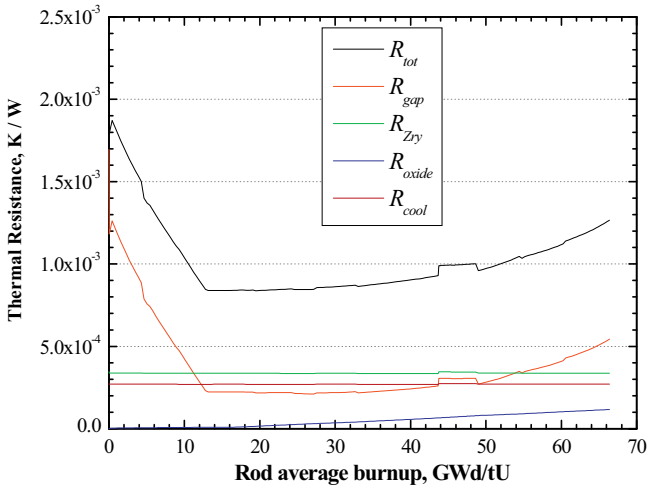


**Fig. 2.** Thermal resistances along irradiation at a location near the bottom of the rod.

$$h_{\text{gap}} = h_{\text{solid}} + \frac{k'_{\text{gas}}}{\delta} \quad (5)$$

Worth to note that the gas conductivity is different in eq. (5) than the initial one (eq. (4)) because of the release of gaseous fission products of lower conductivity than helium (i.e., Xenon and Krypton).

The solid-solid contact occurs through a relatively small fraction of the total surface area. However, given the gap conductance reduction ($h_{\text{gas}}$) and the high contact pressure anticipated at high burn-ups, the solid contact conductance is responsible for most of heat transfer (i.e., $k'_{\text{gas}}/\delta << h_{\text{gap}}$). Therefore, $h_{\text{solid}}$ modelling plays a major role in estimating heat transfer in nuclear fuel rods at high burn-ups.

## 3. Modelling of $h_{\text{solid}}$

Modelling of $h_{\text{solid}}$ in nuclear irradiation codes can be grouped in two major families according to the major hypotheses and approximations taken in the resolution of the heat diffusion equation under steady state conditions: Centinkale and Fishenden family and Mikic family.

### 3.1. The Cetinkale & Fishenden family

The main hypotheses to solve the temperature distribution equation are (Cetinkale and Fishenden, 1951; Lambert and Fletchert, 1997):

- The surface area of apparent contact is divided into $N\cdot(N = 1/(\pi\cdot r_c^2))$ imaginary, equal-sized ($r_c$) and uniformly distributed cylinders.
- Solid-solid contact spots are discs of identical radius ($r_d$).
- Deformations at contact spots are plastic.

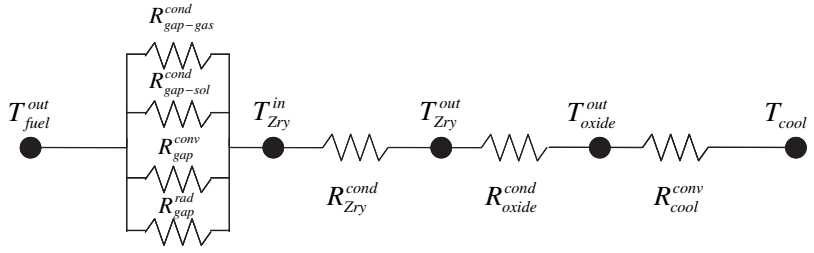


**Fig. 1.** Thermal resistance network from fuel surface to coolant.

Once adapted to high burn-up conditions, the solution found may be written as:

$$h_{solid} = \frac{r_d \cdot k_m}{r_c^2 \cdot \arctan\left(\frac{r_c}{r_d} - 1\right)} \quad (6)$$

The Ross and Stoute (1962) model makes two basic approximations:

- $P_m$ is a fraction of the Meyer Hardness ($H$) of the softer material ($P_m = 0.6 \cdot H$)
- $r_d$ is expressed as a function of the surface roughness (eq. (7))

$$r_d = a_o \cdot \sigma^{0.5} \approx \left(\frac{\sigma_{fuel}^2 + \sigma_{clad}^2}{2}\right)^{\frac{1}{4}} \quad (7)$$

By using these equations together with the expression derived experimentally by Bowden and Tabor (1950) for the ratio (eq. (8)) between the actual and the apparent contact area (eq. (9)):

$$\frac{A_r}{A_a} = \frac{P}{P_m} \quad (8)$$

$$A_a = \pi \cdot r_c^2 \quad (9)$$

($P$ and $P_m$ are the ratio of the force on the interface to the apparent contact area and the actual contact area, respectively), they determined that $h_{solid}$ was directly proportional to the pressure (eq. (10)),

$$h_{solid} = \frac{k_m}{a_o \cdot \sigma^{\frac{1}{2}}} \cdot \frac{P}{H_{clad}} = \alpha \cdot P \quad (10)$$

where $\alpha$ was estimated to be $5 \times 10^{-4}$ W/N-K under nuclear light water reactor operating conditions (MacDonald and Weisman, 1976). The Meyer Hardness in the equation is the one of the cladding one since the zirconium alloy is softer than the uranium pellet.

Lasmann and Pazdera (1983) proposed a slight variation of eq. (10) specifically fitted to those high temperatures anticipated in the fuel-clad contact (eq. (11)),

$$h_{solid} = a_1 \cdot k_m \cdot \sigma \cdot \left(\frac{P}{\sigma^2 \cdot H_{clad}}\right)^m \quad (11)$$

where $a_1$ is an experimental parameter ranging from $0.638 \times 10^6$ and $m$ is roughly 0.69.

Other authors (Rapier et al., 1963) by adopting different approximations obtained other variants of eq. (6), where $h_{solid}$ depended even more mildly on pressure (eq. (12)):

$$h_{solid} = \frac{k_m}{\lambda_{fuel} \cdot \sigma^{\frac{1}{2}}} \cdot \left(\frac{P}{H_{clad}}\right)^{0.5} \quad (12)$$

It should be realized that eq. (12) includes a more detailed surface characterization by accounting of the wavelength of the surface with largest asperities wavelength ($\lambda_{fuel}$).

### 3.2. The Mikic family

Mikic and Roshenow (1966) and Mikic (1974) proposed different assumptions to solve the heat diffusion equation:

- Size of contact spots is variable (function of height and angle of asperities).
- Contact spots are distributed pseudo-uniformly (surface around contact spots is proportional to the contact spot size).
- Elastic and plastic deformations at contact spots are considered.

The result obtained can be expressed as (eq. (13)):

$$h_{solid} = \frac{1.45 \cdot k_m |\overline{\tan\theta}|}{\sigma} \cdot \left(\frac{P}{H_{clad}}\right)^n \quad \begin{array}{ll} n = 0.5 & \text{for plastic flow} \\ n = 1.0 & \text{for elastic flow} \end{array} \quad (13)$$

where $|\overline{\tan\theta}|$ is the average of asperity slopes ($\tan\theta = 2 \cdot \sigma/\lambda$). Data from Jacobs and Todreas (1973) for the particular case of nuclear fuel (i.e., $UO_2$ and Zry) allowed to rewrite the above equation as (eq. (14)):

$$h_{solid} = \frac{5 \cdot k_m}{\sigma} \cdot \left(\frac{P}{H_{clad}}\right)^n \cdot \left(\frac{\sigma_{fuel}}{\lambda_{fuel}}\right) \quad \begin{array}{ll} n = 1.0 & \text{for plastic flow } (P/H) \geq 0.011 \\ (P/H_{clad})^n = 0.01 & 0.0001 < (P/H) < 0.011 \\ n = 0.5 & \text{for elastic flow } (P/H) < 0.0001 \end{array} \quad (14)$$

### 3.3. In codes modelling

The above models, or variants of them, have been implemented in codes simulating nuclear fuel irradiation.

CYRANO 3 code, developed by EDF (1998), adopts the Ross-Stoute approximation in the simplified form of eq. (10),

$$h_{solid} = 50.0 \cdot P \quad (15)$$

where $P$ is in MPa and $h_{solid}$ is in W/m$^2$-K.

Other codes, like URGAP (Lasmann and Pazdera, 1983) and START3 (Bibilashvily et al., 1998), follow the Lasmann approach such as it is defined in eq. (11).

Two of the most extensively used codes, FRAPCON-3 (Lanning et al., 1997) and FALCON (Lyon et al., 2004), adopt the Mikic approach. Their difference lays on the dataset used to fit the model constants. Thus, FRAPCON-3 introduces an alternative form fitted to specific experimental data on $UO_2$ and Zircaloy (Garnier and Begej, 1979) (eq. (16)),

$$\begin{array}{ll} h_{solid} = \frac{0.4166 \cdot k_m}{\sigma} \cdot \left(\frac{P}{H}\right)^{0.5} \cdot \left(\frac{\sigma_{fuel}}{\lambda_{fuel}}\right) & (P/H) < 9 \cdot 10^{-6} \\ h_{solid} = \frac{0.00125 \cdot k_m}{\sigma} \cdot \left(\frac{\sigma_{fuel}}{\lambda_{fuel}}\right) & 0.003 > (P/H) > 9 \cdot 10^{-6} \\ h_{solid} = \frac{0.4166 \cdot k_m \cdot M}{\sigma} \cdot \left(\frac{P}{H}\right) \cdot \left(\frac{\sigma_{fuel}}{\lambda_{fuel}}\right) & (P/H) > 0.003 \end{array} \quad (16)$$

where $M$ is a multiplicative factor (eq. (17)):

$$\begin{array}{ll} M = 333.3 \cdot \left(\frac{P}{H}\right) & \left(\frac{P}{H}\right) \leq 0.0087 \\ M = 2.9 & \left(\frac{P}{H}\right) > 0.0087 \end{array} \quad (17)$$

FALCON, however, uses eq. (14) but the numerical constant is set to 0.5785.

## 4. Parametric analysis

From the previous section one can generally state that the solid-solid conductance is a function of some key parameters (eq. (18)):

$$h_{solid} = f\left(k_{clad}, k_{fuel}, \sigma_{clad}, \sigma_{fuel}, \lambda_{fuel}, P, H\right) \quad (18)$$

In other words, $h_{solid}$ depends on the material properties ($k_i$, $H_i$) , the surface topology ($\sigma_i$, $\lambda_i$) and the contact conditions ($P$). In order to explore and illustrate their influence on $h_{solid}$ a reference scenario representative of in-reactor conditions has been defined (Table 1).

Some properties have been estimated according to updated literature. This is the case of fuel and clad thermal conductivity (eqs. (19) and (20)) (Wiesenack et al., 1996; SCDAP/RELAP CDT, 2003)

$$k_{fuel} = \frac{1}{0.1148 + 0.0035\cdot BU + 2.475\cdot 10^{-4}\cdot\left(1 - 3.33\cdot 10^{-3}\cdot BU\right)\cdot T + 1.32\cdot 10^{-2}\cdot e^{\left(1.88\cdot 10^{-3}\cdot T\right)}} \quad (19)$$

$$k_{clad} = 7.511 + T\cdot\left[2.088\cdot 10^{-2} + T\cdot\left(-1.450\cdot 10^{-5} + T\cdot 7.668\cdot 10^{-9}\right)\right] \quad (20)$$

and Meyer Hardness (eq. (21)) (SCDAP/RELAP CDT, 2003)

$$H_{Zry} = 10^{-6}\cdot\left(26.034 - 0.026394\cdot T + 4.35\cdot 10^{-5}\cdot T^2 - 2.562\cdot 10^{-8}\cdot T^3\right) \quad (21)$$

The results obtained and presented in the next subsections have been individually normalized to the maximum value of each code predictions, so that codes trends can be better analysed.

### 4.1. Effect of contact pressure

All the code equations consider contact (or interfacial) pressure as one of the main variables. Under high burn-up conditions, contact pressures can reach values around 40 MPa (Jernkvist and Massih, 2004) or even higher. The data shown in Fig. 3 reach 50 MPa, but it should be stressed that some of the predictions are just extrapolations out of the applicability range (for instance, the applicability range of FRAPCON-3 code correlation is limited to around 27 MPa).

At the high burn-up pressure range (25–50 MPa), all the codes show a linear trend except for START3 which encapsulates an $h_{solid}$ dependence with $P$ a bit milder ($\alpha\cdot P^{0.69}$). Hence, no major discrepancies exist under at high burn-up on the way $P$ influence on $h_{solid}$ is implemented in the codes.

### 4.2. Effect of interfacial temperature

Interfacial temperature affects $h_{solid}$ through the materials conductivity and Zircaloy hardness. However, in the temperature range of interest (i.e., 600–800 K) materials conductivity variation

**Table 1**
Reference scenario of the parametric analysis.

| | | |
|---|---|---|
| $BU$ | 70 (60–80) | GWd/t |
| $P$ | 15 | MPa |
| $T$ | 700 (600–800) | K |
| $\sigma_{fuel}$ | $1.6 \times 27\ 10^{-6}$ | m |
| $\sigma_{clad}$ | $0.4 \times 10^{-6}$ | m |

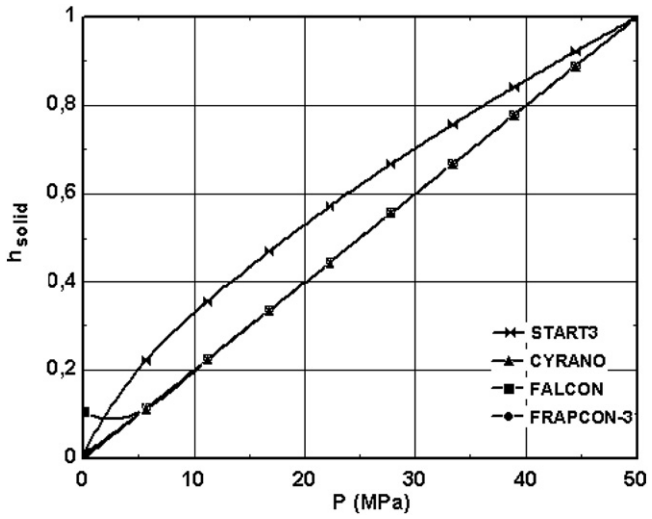


**Fig. 3.** $h_{solid}$ as a function of the interfacial pressure ($T = 700$ K).

is responsible for hardly a 6% change in the mean thermal conductivity ($k_m$). On the other hand, Zircaloy hardness experiences a reduction of roughly 50% as temperature rises from 600 K to 800 K. Therefore, $h_{solid}$ sensitivity to interfacial temperature observed in Fig. 4 is mostly driven by Zircaloy Meyer hardness ($H_{Zry}$).

FALCON and FRAPCON influence of interfacial temperature is exactly the same, whereas START3, even though behaves similarly, shows less sensitivity to interfacial temperature. The CYRANO code is the only one which neglects the $h_{solid}$ dependence on $T$, which is not suitable since, as observed, in the temperature range of interest, $h_{solid}$ could even double.

This study highlights that, except for the CYRANO code, the codes response to interfacial temperature changes is quite the same.

### 4.3. Effect of surface morphology

Waviness and roughness characterize surface morphology. According to Edmonds et al. (1980), waviness dominates the surface effect at low contact pressures, whereas roughness does at high ones.

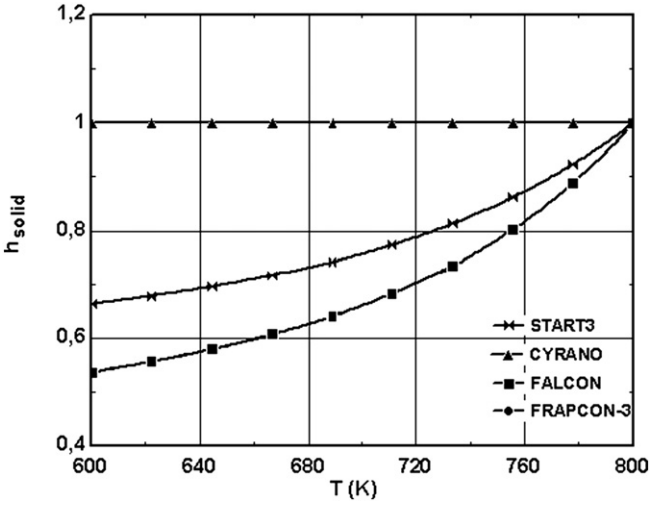


**Fig. 4.** $h_{solid}$ as a function of the interfacial temperature ($P = 15$ MPa).

FRAPCON-3 and FALCON codes correlate fuel waviness and roughness (eq. (22)),

$$\left(\frac{\sigma_{\text{fuel}}}{\lambda_{\text{fuel}}}\right) = \frac{1}{\exp\left(5.738 - 0.528\cdot\ln\left(\sigma_{\text{fuel}}\right)\right)} \tag{22}$$

so that, eventually, all the codes being explored, except for CYRANO 3, encapsulate the influence of morphology on $h_{\text{solid}}$ through material surface roughness exclusively (i.e., $\sigma_{\text{fuel}}$ and $\sigma_{\text{clad}}$). Differences in $h_{\text{solid}}$ sensitivity to surface characterization in FALCON, FRAPCON-3 and START3 should be brought up by their different dependency on $\sigma_{\text{fuel}}$ since all of them consider $\sigma_{\text{clad}}$ in the same way.

There are few data on those parameters in the open literature (Jacobs and Todreas, 1973; Madhusana, 1980; Lanning et al., 1997) and, although they usually extend over a broad spectrum, $UO_2$ and Zircaloy roughness use to be in the range of sub-micron to few microns. As a consequence, the range of the root-mean-square roughness ($\sigma$) explored in this study was 1–20 μm.

Fig. 5 shows the variation of $h_{\text{solid}}$ with the root-mean-square roughness. Worth to note that, except for the CYRANO code, the rest of codes show the same kind of dependence with no significant quantitative discrepancies (in particular, FRAPCON-3 and FALCON have exactly the same evolution, as expected from respective equations). In other words, the effect of surface morphology in codes predictions is substantial ($h_{\text{solid}}$ can decrease by a factor of 10 in the range of interest), but not major discrepancies in codes predictions should come from this sensitivity (except for the CYRANO code, which lacks this dependency).

In any case, morphology of the contact surfaces is claimed not to be relevant at high burn-ups (Chantoin et al., 1998), where the gap is anticipated to be closed. In addition, both fuel and cladding surface states after long irradiation periods are uncertain. The rim formation in the fuel and the chemical attack of inner cladding by some fission products, are expected to change drastically their initial conditions.

Therefore, as indicated above concerning contact pressure and interfacial temperature, surface morphology should not be highlighted as a major source of discrepancies in code predictions, except for the case of the CYRANO code.

### 4.4. Absolute values comparison

From the above subsections one can conclude that most of the codes (except for CYRANO) encapsulate identical or similar variable dependencies in $h_{\text{solid}}$ under the conditions expected under high burn-up. Hence, the discrepancies shown in Fig. 6 as absolute values, come essentially from the numerical parameters embedded in $h_{\text{solid}}$ equations. In other words, predictions differences result from the fact different dataset have been used for validation of in-code equations for $h_{\text{solid}}$.

Two different FRAPCON-3 calculations have been included, depending on whether the $M$ factor is considered ($a$) or not ($b$). Noteworthy that as $M$ is set to 1.0, FRAPCON-3 practically coincides with CYRANO (pure linear behaviour) for the whole range of pressures analysed.

The results in Fig. 6 and the preceding discussion raise a major point: data reliability and representativity of high burn-up conditions. On the reliability issue, data sets typically exhibit a large scatter; a characteristic scatter around a factor of 2.0 is usual in the data from Garnier and Begej (1979) and Ross and Stoute (1962), regardless the pressure. This means that the best correlation possible will have anyway low correlation coefficients (Lasmann and Pazdera, 1983); so to say, predictions from those correlations will have a large uncertainty range. On the representativity issue, most of data used to develop and validate the in-code models were recorded decades ago, when fuel burn-up was much lower. Thus, shortcomings come from two sources: the limitation of the range under which samples were tested (as in the case of Garnier which pressure range did not even reach 25 MPa) and the importance of the changes resulting from high burn-up, such as the mechanical degradation of the fuel rim (Spino et al., 1996), that could considerably affect the fuel-clad contact.

## 5. Data-predictions comparison

Solid-solid conductance of nuclear fuel and cladding has been scarcely measured experimentally. What's more, some of those researches are not open. The present comparison is restricted to those available data that were obtained under similar conditions to those anticipated under high burn-up. Cross and Fletcher (1978) investigated the temperature effect under too low contact pressures (0.25–0.79 MPa) and temperatures (27–74 °C). Madhusana (1980) measured the effect of pressure in the range of 2–20 MPa, which is still too low for high burn-up situations. Jacobs and Todreas (1973) compiled a good number of data recorded by other investigators, but just few of them could be seen as representative of high burn-up conditions.

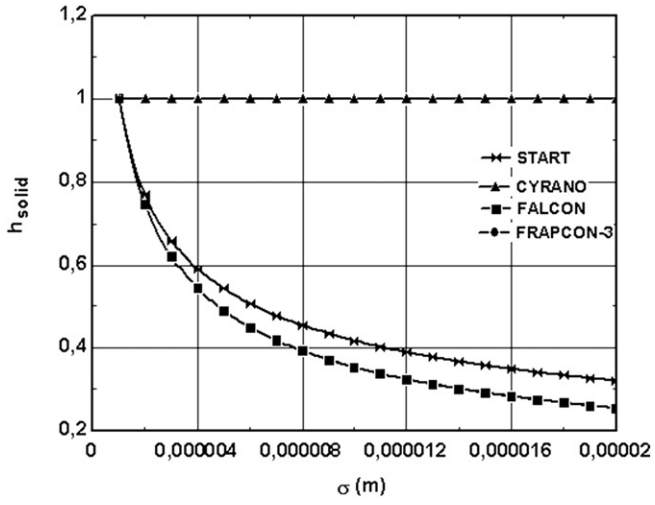


**Fig. 5.** $h_{\text{solid}}$ as a function of root-mean-square roughness ($\sigma_{\text{clad}} = 0.4 \times 10^{-6}$ μm).

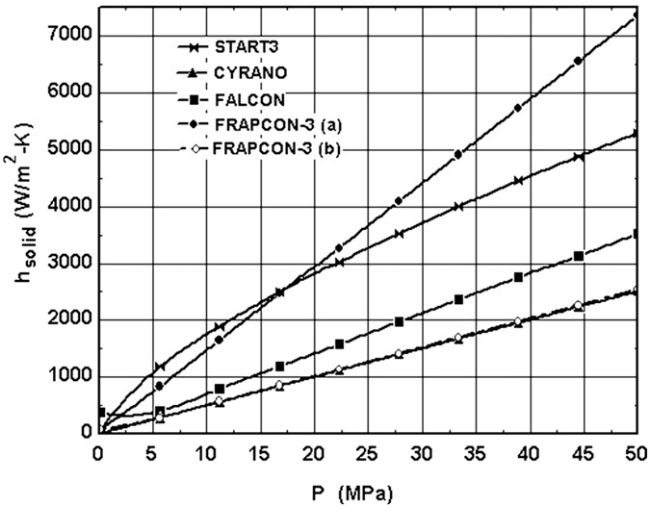


**Fig. 6.** $h_{\text{solid}}$ as a function of the interfacial pressure.

An experimental data set has been built-up to compare to in-code models predictions. Two major criteria were adopted for test selection: high contact pressure (20–50 MPa) and materials root-mean-square roughness around 1 μm. A total of 8 test cases from the data base of Ross and Stoute for $UO_2$-Zircaloy 2 have been chosen (Table 2). As interface temperature was not reported, temperature is assumed to be the one resulting in the best agreement between data and START3 predictions (which parameters were fitted to Ross data) for the highest pressure of each fuel roughness value.

In Table 3 the relative error (%) of predictions are gathered. As noted, most of codes tend to underestimate the contact conductance at low pressures and small fuel roughness. This observation was discussed by Milanez et al. (2004) to be the result of approximating roughness size by a normal distribution, which tends to overestimate roughness height; they conclude that such an approximation become more accurate as contact pressures are higher (i.e., high burn-up).

START3 predictions, as expected, showed a small error. More remarkable, the calculations of FRAPCON-3 have shown an outstanding agreement to data, the average error being around 18.4%. As said above, this is well within the experimental scatter observed in most of data. The FALCON and CYRANO codes predictions underestimate notably the experimental data, particularly CYRANO which average error is around 74.8%.

By plotting the normalized conductance versus contact pressure (Fig. 7), FRAPCON-3 and START3 predictions are compared to data (worth to recall that FALCON and CYRANO had the same behaviour as FRAPCON-3 with respect to contact pressure). The trend of both code predictions are bracketed between data of different root-mean-square roughness. Apparently, sensitivity to contact pressure is linked to materials roughness; however, in-code models do not encapsulate that connection. This is clearly observed in Table 4, where absolute $h_{solid}$ data show that the ratio of $h_{solid}$ corresponding to 0.7 and 1.4 μm roughness, change with pressure, whereas FRAPCON-3 estimates do not experience any change. Even though ratio values almost coincide at around 50 MPa, the predictions constancy as well as the data decrease seems to point out that higher contact pressures would drive to less data sensitivity to roughness than model's one. Thus, roughness-pressure connection is missing within in-code models.

## 6. Final remarks

Along this paper fundamentals and sensitivity of solid-solid conductance models used in nuclear safety codes have been reviewed and their adequacy to anticipated high burn-up conditions has been discussed. Next, the major insights gained are summarised:

- The in-code models group in two sets according to different hypotheses and approximations made regarding material behaviour and interaction in the resolution of the general diffusion equation. Nonetheless, except for CYRANO 3, all of them depend on contact pressure and temperature and roughness of material surfaces.
- The CYRANO 3 code formulation is extremely simple. This makes it useful as a fast-running code, but makes it unable to follow the experimental trends observed with temperature and roughness. However, as it noticeably underestimates data, its predictions are conservative from the safety point of view.
- The START3 code shows consistent responses to the variation of governing variables, although it seems to be a bit less sensitive than the Mikic family codes (i.e., FRAPCON-3 and FALCON).
- The FRAPCON-3 and FALCON codes present exactly the same sensitivity to the major scenario variables, particularly under high burn-up conditions. However, they differ in the quantitative predictions, the FRAPCON-3 estimates being higher than FALCON ones in around a factor of 2.0. This discrepancy is partially associated to the FRAPCON-3 factor (M) introduced in FRAPCON to fit the Garnier and Begej (1979) data.
- The FRAPCON-3 code results are the most accurate ones when compared to the dataset built-up from the available data that can be considered representative of high burn-up. The FALCON and CYRANO code predictions are notably less accurate, but their accuracy is anyway within the experimental scatter.

In summary, nuclear safety codes encapsulate major variables governing solid-solid conductance and their trends look consistent. Even though the reduced number of data does not allow to settle general conclusions about model performance, substantial discrepancies have been found in their predictions. They have highlighted two important facts: the large scattering of already

**Table 2**
Data set for comparison purposes with in-code models predictions.

| Test case | Roughness (μm) | | $P$ (MPa) | $h$ (W/m$^2$-K) |
|---|---|---|---|---|
| | Fuel | Cladding | | |
| 1 | 0.31 | 0.62 | 19.1 | 9113.7 |
| 2 | 0.31 | 0.62 | 29.1 | 11981.2 |
| 3 | 0.31 | 0.62 | 39.1 | 13003.3 |
| 4 | 0.31 | 0.62 | 48.1 | 14025.4 |
| 5 | 1.25 | 0.62 | 19.1 | 2501.4 |
| 6 | 1.25 | 0.62 | 29.1 | 4099.7 |

**Table 3**
Relative error of predictions (%).

| Test Case | START3 | FRAPCON-3 | FALCON | CYRANO |
|---|---|---|---|---|
| 1 | −15.3 | −27.8 | −65.4 | −89.5 |
| 2 | −18.8 | −16.3 | −60.0 | −87.9 |
| 3 | −2.6 | 3.6 | −50.4 | −85.0 |
| 4 | 5.6 | 20.6 | −42.3 | −82.5 |
| 5 | 47.0 | 24.7 | −40.3 | −61.7 |
| 6 | 20.0 | 16.0 | −44.5 | −64.5 |
| 7 | 16.1 | 23.0 | −41.1 | −62.4 |
| 8 | 1.1 | 14.9 | −45.0 | −64.8 |

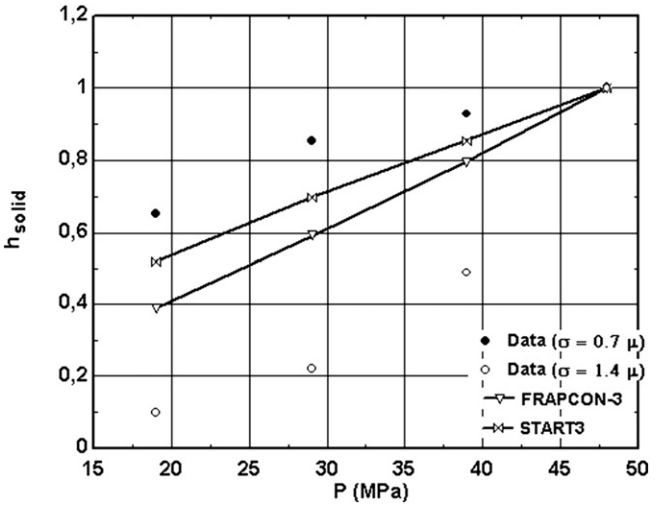


**Fig. 7.** Data-predictions comparison of normalized conductance versus contact pressure.

**Table 4**
$h_{solid}$ sensitivity to materials roughness as a function of contact pressure.

| Pressure (MPa) | Data | | | FRAPCON-3 predictions | | |
|---|---|---|---|---|---|---|
| | $h_{solid}$ (W/m$^2$ K) | | Ratio | $h_{solid}$ (W/m$^2$ K) | | Ratio |
| | $\sigma = 0.7$ μm | $\sigma = 1.4$ μm | | $\sigma = 0.7$ μm | $\sigma = 1.4$ μm | |
| 19.1 | 9113.7 | 2504.1 | 3.6 | 6579 | 3122 | 2.1 |
| 29.1 | 11981.2 | 4099.7 | 2.9 | 10,023 | 4756 | 2.1 |
| 39.1 | 13003.3 | 5195.6 | 2.5 | 13,467 | 6391 | 2.1 |
| 49.0 | 14025.4 | 6984.3 | 2.0 | 16,911 | 8025 | 2.1 |

available data base and the scarcity of data under anticipated high burn-up conditions.

Therefore, from the scientific point of view, experimental work on heat transfer through the fuel-clad interface under conditions anticipated at high burn-up is highly recommended. Use of accurate experimental techniques and methods would be extremely important to decrease data scattering. Nonetheless, from the safety point of view, an importance analysis should be carried out a priori to assess the actual effect of solid-to-solid modelling uncertainties in the overall fuel-to-coolant heat transfer modelling at high burn-up conditions.

## Appendix. Nomenclature

| | |
|---|---|
| $A$ | surface area |
| $a_o$ | empirical constant |
| $a_1$ | empirical constant |
| $BU$ | burn-up |
| $H$ | Meyer Hardness of cladding |
| $k$ | thermal conductivity |
| $k_m$ | mean thermal conductivity of solids ($k_m = (2 \cdot k_{clad} \cdot k_{fuel})/(k_{fuel} + k_{clad})$) |
| $L$ | characteristic length |
| $P$ | pressure (ratio of interfacial force to apparent contact area) |
| $P_m$ | pressure (ratio of interfacial force to actual contact area) |
| $\dot{q}'$ | linear heat generation rate |
| $r$ | radius |
| $R$ | thermal resistance |
| $T$ | temperature |

*Subindex*

| | |
|---|---|
| a | apparent |
| c | cylinder |
| clad | cladding |
| cond | conduction |
| conv | convection |
| cool | coolant |
| d | disc |
| fuel | fuel |
| gap | gap |
| gas | gas |
| oxide | oxide |
| rad | radiation |
| solid | solid |
| Total | total |
| Zry | Zircaloy |

*Greek symbols*

| | |
|---|---|
| $\alpha$ | experimental constant |
| $\delta$ | gap width |
| $\lambda$ | surface asperity wavelength |
| $\sigma$ | roughness |
| $\theta$ | angle of asperity slope |

## References


Bibilashvily, U.E., Medvedev, A.V., Bogatyr, S.I., Kouznetsov, V.I., Khvostov, G.À., 1998. START-3 code gap conductance modelling. In: Proceedings of the Seminar On: Thermal Performance of High Burn-up LWR Fuel, Cadarache, France.

Bowden, F.P., Tabor, D., 1950. The Friction and Lubrication of Solids. Clarendon Press, Oxford.

Cayet, N., Baron, D., Beguin, S., 1998. Cyrano 3: EDF's Fuel Rod Behaviour Code-presentation and Overview of its Qualification on HRP and various other Experiments. Enlarged Halden Reactor Project Meeting, Lillehammer, Norway 1998. Paper also presented in the Thermal Performace LWR fuel Sminar, Cadrache, France, 1998.

Cetinkale, T.N., Fishenden, M., 1951. Thermal conductance of metal surfaces in contact. In: International Conference of Heat Transfer, London.

Chantoin, P.M., Sartori, E., Turnbull, J.A., 1998. The compilation of a public domain database on nuclear fuel performance for the purpose of code development and validation. In: ANS Topical Meeting on Light Water Reactor Fuel Performance, Portland, USA.

Cross, R.W., Fletcher, L.S., 1978. Thermal Contact Conductance of Uranium Dioxide Zircaloy Interfaces. Departement of Mechanical and Aerospae Engineering, Universiry of Virginia.

Edmonds, M., Jones, A.M., Probert, S.D., 1980. Thermal contact resistance of hard machined surfaces pressed against relatively soft optical flats. Applied Energy 6, 405–427.

Garnier, J.E., Begej, S., 1979. Ex-reactor Determination of Thermal Gap and Contact Conductance Between Uranium Dioxide: Zircaloy-4 Interfaces. Stage I: Low Gas Pressure, NUREG/CR-0330.

Godesar, R., 1972. Untersuchungen des Einflusses des Wärmeübergagskoeffizientzn im Spalt zwischen Brestöff and Hülle auf die sicher, Dissertation PhD, Aachen.

Herranz, L.E., Vallejo, I., del Barrio, M.T., 2003. Análisis of the effect of the FRAPCON-3 approximation regarding cladding thickness change onto fuel-coolant heat transfer under high burnup scenarios. In: The Tenth International Topical Meeting on Nuclear Reactor Thermal Hydraulics (NURETH-10), October 5–9, 2003, Seoul, Korea.

Jacobs, G., Todreas, N., 1973. Thermal contact conductance in reactor fuel elements. Nuclear Science and Engineering 50, 283–306.

Jernkvist, L.O., Massih, A.R., 2004. Models for Fuel Rod Behaviour at High Burn-up SKI Report 2005–41.

Lambert, M.A., Fletchert, L.S., 1997. Review of models for thermal contact conductance of metals. Journal of Thermophysics and Heat Transfer 11, 2. April–June.

Lanning, D.D., Beyer, C.E., Berna, G.A., Davis, K.L., 1997. Frapcon 3: A Computer Code for the Calculation of Steady state, Thermal Mechanical Behaviour of Oxide Fuel Rods for High Burn-Up. NUREG-Vol 2- PNNL-11513.

Lasmann, K., Pazdera, F., 1983. URGAP: a gap conductance model for transient conditions. In: Gittus, J. (Ed.), Water Reactor Fuel Element Performance Computer Modelling. Appl. Science Publishers LTD, England, pp. 97–113.

Lyon, W.F., Jahingir, N., Montgomery, R.O., Yagnik, S., 2004. Capabilities of the FALCON steady state and transient fuel performance code. In: 2004 International Meeting on LWR Fuel Performance. Fuel Reliability: Successes and Challenges, Orlando, US.

MacDonald, P.E., Weisman, J., 1976. Effect of pellet cracking on light water reactor fuel temperatures. Nuclear Technology 31, 357–366.

Madhusana, C.V., 1980. Experiments on heat flow through Zircaloy-2/uranium dioxide surfaces in contact. Journal of Nuclear Materials 92, 345–348.

Mikic, B., 1974. Thermal contact conductance: theoretical considerations. International Journal of Heat Mass Transfer 17, 205–214.

Mikic, B., Roshenow, 1966. Thermal Contact Resistance. DRS 74542-41. Mechanical Engineering Departament, MIT.

Milanez, H., Yovanovich, J.R., Mantelli, H., 2004. Thermal contact conductance at low contact pressures. Journal of Thermophysics and Heat Transfer 18 (1).

Rapier, A.C., Jones, T.M., McIntosh, J.E., 1963. The thermal conductance of uranium dioxide/stainless steel interfaces. International Journal of Heat Mass Transfer 6, 397–416.

Ross, A.M., Stoute, R.L., 1962. Heat Transfer Coefficient Between $UO_2$ and Zircaloy 2 AECL-1552.

SCDAP/RELAP Code Development Team, 2003. MATPRO – A Library of Materials Properties for Light-Water-Reactor Accident Analysis INEEL/EXT-02–00589.

Spino, J., Vennix, K., Coquerelle, M., 1996. Detailed characterization of the rim structure in PWR fuels in the burnup range 40–67 GWd/tU. Journal of Nuclear Materials 231, 179–190.

Wiesenack, W., Vankeerberghen, M., Thankappan, R., 1996. Modelling of $UO_2$ Conductivity Degradation Based on In-pile Temperature Data HWR-469.